ACBD3 Interaction with TBC1 Domain 22 Protein Is Differentially Affected by Enteroviral and Kobuviral 3A Protein Binding

Alexander L. Greninger, Giselle M. Knudsen, Miguel Betegon, et al.

2013. ACBD3 Interaction with TBC1 Domain 22 Protein Is Differentially Affected by Enteroviral and Kobuviral 3A Protein Binding. mBio 4(2): . doi:10.1128/mBio.00098-13.

RESEARCH ARTICLE

ACBD3 Interaction with TBC1 Domain 22 Protein Is Differentially Affected by Enteroviral and Kobuviral 3A Protein Binding

Alexander L. Greninger,[a,b] Giselle M. Knudsen,[c] Miguel Betegon,[a,b] Alma L. Burlingame,[c] Joseph L. DeRisi[a,b]

Howard Hughes Medical Institute, San Francisco, California, USA[a]; Department of Biochemistry and Biophysics, UCSF, San Francisco, California, USA[b]; Department of Pharmaceutical Chemistry, UCSF, San Francisco, California, USA[c]

ABSTRACT Despite wide sequence divergence, multiple picornaviruses use the Golgi adaptor acyl coenzyme A (acyl-CoA) binding domain protein 3 (ACBD3/GCP60) to recruit phosphatidylinositol 4-kinase class III beta (PI4KIIIβ/PI4KB), a factor required for viral replication. The molecular basis of this convergent interaction and the cellular function of ACBD3 are not fully understood. Using affinity purification-mass spectrometry, we identified the putative Rab33 GTPase-activating proteins TBC1D22A and TBC1D22B as ACBD3-interacting factors. Fine-scale mapping of binding determinants within ACBD3 revealed that the interaction domains for TBC1D22A/B and PI4KB are identical. Affinity purification confirmed that PI4KB and TBC1D22A/B interactions with ACBD3 are mutually exclusive, suggesting a possible regulatory mechanism for recruitment of PI4KB. The C-terminal Golgi dynamics (GOLD) domain of ACBD3 has been previously shown to bind the 3A replication protein from Aichi virus. We find that the 3A proteins from several additional picornaviruses, including hepatitis A virus, human parechovirus 1, and human klassevirus, demonstrate an interaction with ACBD3 by mammalian two-hybrid assay; however, we also find that the enterovirus and kobuvirus 3A interactions with ACBD3 are functionally distinct with respect to TBC1D22A/B and PI4KB recruitment. These data reinforce the notion that ACBD3 organizes numerous cellular functionalities and that RNA virus replication proteins likely modulate these interactions by more than one mechanism.

IMPORTANCE Multiple viruses use the same Golgi protein (ACBD3) to recruit the lipid kinase phosphatidylinositol 4-kinase class III beta (PI4KB) in order to replicate. We identify a new binding partner of ACBD3 in the evolutionarily conserved Rab GTPase-activating proteins (RabGAPs) TBC1D22A and -B. Interestingly, TBC1D22A directly competes with PI4KB for binding to the same location of ACBD3 by utilizing a similar binding domain. Different viruses are able to influence this interaction through distinct mechanisms to promote the association of PI4KB with ACBD3. This work informs our knowledge of both the physical interactions of the proteins that help maintain metazoan Golgi structure and how viruses subvert these evolutionarily conserved interactions for their own purposes.

Received 7 February 2013 **Accepted** 8 March 2013 **Published** 9 April 2013

Citation Greninger AL, Knudsen GM, Betegon M, Burlingame AL, DeRisi JL. 2013. ACBD3 interaction with TBC1 domain 22 protein is differentially affected by enteroviral and kobuviral 3A protein binding. mBio 4(2):e00098-13. doi:10.1128/mBio.00098-13.

Invited Editor Julie Pfeiffer, University of Texas Southwestern Medical Center **Editor** Terence Dermody, Vanderbilt University School of Medicine

Address correspondence to Joseph L. DeRisi, joe@derisilab.ucsf.edu.

Picornaviruses are single-stranded positive-sense RNA viruses that replicate on intracellular membranes (1). Previous work has indicated that the 3A protein is responsible for the reorganization of Golgi membranes to create viral replication organelles (2, 3). The molecular basis of this reorganization has only recently become apparent through the dual discoveries that enteroviral 3A directly interacts with Golgi-specific brefeldin A resistance guanine nucleotide exchange factor 1 (GBF1) and that many RNA viruses require the activity of phosphatidylinositol 4-kinase class III beta (PI4KB) for viral replication (2, 3). However, many questions remain, as not all picornaviruses that require PI4KB activity interact with GBF1, and the portion of GBF1 required for viral replication appears independent of its known Arf1 guanine exchange activity (4).

Two protein-protein interaction screens recently demonstrated that the 3A proteins of enteroviruses and kobuviruses both interact with the host Golgi adaptor protein acyl coenzyme A (acyl-CoA) binding domain protein 3 (ACBD3/GCP60) to recruit PI4KB to viral replication organelles (5, 6). ACBD3 is a highly conserved Golgi complex-associated 60-kDa protein among metazoans that contains a remarkably long N-terminal acyl-CoA binding domain, a coiled-coil domain composed of a charged amino acid region (CAR) and glutamine-rich region (Q-rich), and a highly conserved C-terminal Golgi dynamics domain (GOLD domain) that interacts with the Golgi resident protein giantin/GOLGB1 (7). The level of expression of ACBD3 has been shown to be important for the maintenance of the Golgi structure (7). The picornavirus 3A-ACBD3 interaction is required for replication, as knockdown of ACBD3 significantly reduces poliovirus and Aichi virus replication (5, 6). Furthermore, mutations that reduce binding of Aichi virus 3A to ACBD3 sensitize virus to PI4KB inhibitors, suggesting that recruitment of PI4KB is mediated by the 3A-ACBD3 interaction (5). Intriguingly, a recent yeast two-hybrid screen of hantavirus nonstructural proteins also dem-

onstrated a physical interaction with ACBD3, suggesting that this protein may be broadly required for viral replication due to its native association with PI4KB (8). Further study of the cellular function of ACBD3 is warranted to better understand its role in viral replication and its potential as a target for therapeutic intervention.

In this study, we used affinity purification-mass spectrometry (AP-MS) to identify new protein-protein interactions of ACBD3. We discovered a new interaction with the putative Rab33 GTPase-activating protein (GAP) TBC1D22A/B (9). Detailed mapping of the ACBD3 interactome revealed a mutually exclusive interaction between PI4KB and TBC1D22A/B for a highly conserved region in the coiled-coil domain of ACBD3. While picornaviral 3A proteins bind to the C-terminal GOLD domain on ACBD3, we also find that the enterovirus and kobuvirus 3A proteins interact with ACBD3 in a functionally distinct manner based on differential displacement of TBC1D22A/B, isolation of an ACBD3 mutant that displays differential binding between the 3A proteins, and different ACBD3 binding sites on the 3A proteins.

RESULTS

AP-MS of Strep-tagged ACBD3 reveals interaction with TBC1D22A/B. Based on its identification as a specific protein interaction partner for picornavirus 3A proteins, the multifunctional protein ACBD3 was hypothesized to be used by 3A as an organizing-scaffold protein at the Golgi interface. To identify potential novel interactions of ACBD3 relevant to the 3A system in host cells, we transiently overexpressed and affinity purified N- and C-terminally StrepII-tagged ACBD3 in 293T cells and identified interacting proteins by mass spectrometry (Table 1; see also Tables S1, Tab SI.3A and SI.4 in the supplemental material). Nonspecific interacting proteins were defined as the highest-frequency proteins identified in a background model of 550 AP-MS data sets compiled from the structural and nonstructural genes from 12 different picornaviruses, excluding the 3A protein itself (see Table S1, Tab SI.1).

Using this AP-MS approach combined with *Z* score ranking for interaction specificity, we found that ACBD3 interacted with the TBC1 domain family member 22A protein (TBC1D22A) in a highly specific manner and at levels that were comparable to those of PI4KB (Table 1; full *Z* scores are provided in Table S1, Tab SI.4 in the supplemental material). Additional proteins such as transmembrane protein 55B isoform 2 (TMEM55B) and protein phosphatase 1H (PPM1H) were also observed to be specific for ACBD3. The known ACBD3-interacting Golgi protein giantin/GOLGB1 was identified in affinity purifications of N-terminally tagged ACBD3 only in a buffer that included potassium chloride and divalent cations (Table 1) (7).

TBC1D22A is a 58-kDa protein that is localized to the Golgi apparatus and involved in Golgi membrane maintenance, along with its closely related isoform TBC1D22B (10). Both contain a C-terminal TBC domain that is responsible for Rab GTPase activation with a putative preference for Rab33A/B (9). Overexpression of TBC1D22B was shown to cause disruption of the endoplasmic reticulum (ER)-Golgi intermediate compartment (ERGIC), which was dependent on its GTPase-activating protein (GAP) activity (10). Based on the localization of ACBD3 and picornavirus replication to ERGIC-associated membranes, TBC1D22A/B merited further investigation.

Affinity purification of TBC1D22A/B or PI4KB captures ACBD3 and 14-3-3 proteins. To confirm the ACBD3-TBC1D22A interaction, reciprocal affinity purification was undertaken with N- and C-terminally Strep-tagged TBC1D22A and TBC1D22B (see Table S1, Tab SI.3A and SI.3B in the supplemental material). The top-ranking interacting protein for both TBC1D22A and TBC1D22B was ACBD3 (Table 1). Multiple 14-3-3 isoforms were also found in high abundance in affinity purifications for both TBC1D22A and TBC1D22B (see Table S1, Tab SI.5). 14-3-3 proteins are 27-kDa adaptor proteins that bind phosphoserine residues on a multitude of cellular proteins involved in diverse signaling pathways (11). TBC1D22A/B phosphopeptides are reported in Table S1, Tab SI.6 and include a putative 14-3-3 recognition site at serine 167 (TBC1D22A) or serine 154 (TBC1D22B; spectra are provided in Fig. S1). No peptides for PI4KB were recovered in any AP-MS experiments on TBC1D22A or TBC1D22B, suggesting that ACBD3-TBC122A/B-containing complexes do not contain PI4KB.

To further confirm the PI4KB-ACBD3 interaction, affinity purification of Strep-tagged PI4KB was performed. The top-ranking protein was ACBD3, while a 14-3-3 isoform was ranked third (Table 1; see also Table S1, Tab SI.3D in the supplemental material). The 14-3-3 proteins have been shown to bind PRKD1-phosphorylated serine 294 of PI4KB and influence its catalytic activity (12). This phosphorylated site and others were identified in our affinity purifications as well, as reported in Table S1, Tab SI.6 (spectrum is provided in Fig. S1). Several additional proteins of unknown significance (C10orf76, GBA, and MTA2) discovered in a recent Flag tag AP-MS experiment on PI4KB also ranked highly in our screen (13). Finally, as in the reciprocal case above, no peptides for TBC1D22A or TBC1D22B were recovered in any AP-MS experiments on PI4KB.

ACBD3-TBC1D22A/B interaction maps to coiled-coil region and overlaps with PI4KB-interacting region of ACBD3. To further query the hypothesis that TBC1D22A/B binding and PI4KB binding may represent distinct, potentially competitive binding states of ACBD3, a mammalian two-hybrid reporter assay was used to map the sites of interaction on ACBD3 by deletion mutagenesis (Fig. 1). N-terminal truncations of the acyl-CoA binding domain, C-terminal truncations of the GOLD domain, and alanine scanning through the entirety of the CAR domain did not affect ACBD3 binding to TBC1D22A/B, while deletions and point mutations located in the conserved glutamine-rich coiled-coil region between residues 246 and 321 significantly reduced TBC1D22A/B binding (see Fig. S2 and S3 in the supplemental material; also Fig. 1). This region has previously been implicated in binding PI4KB (6). Mapping of PI4KB on ACBD3 revealed significant overlap with the region bound by TBC1D22A/B (Fig. 1A). Three mutants with mutations in the glutamine-rich region (VQF255AAA, PGN267AAA, and EQHY281AAAA) significantly reduced ACBD3 binding to both PI4KB and TBC1D22A/B (Fig. 1B; see also Fig. S2B). However, we could isolate no mutant of ACBD3 that retained wild-type levels of PI4KB binding while disrupting TBC1D22A/B binding, or vice versa, including mutation of a recovered phosphorylation site, SS344 (see Table S1, Tab SI.6). Two single point mutants in the glutamine-rich region (F258A and Y285A) did demonstrate a significant difference in PI4KB binding versus TBC1D22B and merit further investigation (Fig. S3). Although we have mapped the critical binding region of TBC1D22A/B to the Q-rich region of ACBD3, we cannot discount

TABLE 1 Interacting proteins identified by AP-MS for ACBD3, TBC1D22A, TBC1D22B, and PI4KIIIb[a]

Bait	Ca^{2+}	Accession no.	Gene designation	Protein name	*Z* score	Replicate count sum
ACBD3 NS	−	15826852	ACBD3	Golgi resident protein GCP60	23.5	699
ACBD3 NS	−	22507409	TBC1D22A	TBC1 domain family member 22A	23.5	13
ACBD3 NS	−	154816184	TMEM55B	Transmembrane protein 55B isoform 2	19.5	11
ACBD3 NS	−	311771621	PI4KB	Phosphatidylinositol 4-kinase beta isoform 2	15.6	5
ACBD3 CS	−	15826852	ACBD3	Golgi resident protein GCP60	23.5	587
ACBD3 CS	−	154816184	TMEM55B	Transmembrane protein 55B isoform 2	19.5	6
ACBD3 CS	−	149944715	PPM1H	Protein phosphatase 1H	15.6	14
ACBD3 CS	−	22507409	TBC1D22A	TBC1 domain family member 22A	11.7	12
ACBD3 CS	−	311771621	PI4KB	Phosphatidylinositol 4-kinase beta isoform 2	7.8	6
ACBD3 NS	+	15826852	ACBD3	Golgi resident protein GCP60	23.5	701
ACBD3 NS	+	148596984	GOLGB1	Golgin subfamily B member 1	23.5	62
ACBD3 NS	+	83641874	CPVL	Probable serine carboxypeptidase CPVL precursor	23.5	21
ACBD3 NS	+	154816184	TMEM55B	Transmembrane protein 55B isoform 2	23.5	17
ACBD3 NS	+	11386135	BCKDHA	2-Oxoisovalerate dehydrogenase subunit alpha, mitochondrial isoform 1 precursor	15.6	27
ACBD3 NS	+	34101272	BCKDHB	2-Oxoisovalerate dehydrogenase subunit beta, mitochondrial precursor	15.6	13
ACBD3 NS	+	38026892	ALG6	Dolichyl pyrophosphate Man9GlcNAc2 alpha-1,3-glucosyltransferase precursor	15.6	12
ACBD3 NS	+	19923748	DLST	Dihydrolipoyllysine residue succinyltransferase component of 2-oxoglutarate dehydrogenase complex, mitochondrial isoform 1 precursor	15.6	8
ACBD3 NS	+	124494254	PA2G4	Proliferation-associated protein 2G4	11.7	7
ACBD3 NS	+	7019485	PDCD6	Programmed cell death protein 6	11.7	7
ACBD3 NS	+	311771621	PI4KB	Phosphatidylinositol 4-kinase beta isoform 2	11.7	6
ACBD3 NS	+	6912582	PEF1	Peflin	11.7	6
ACBD3 NS	+	55741641	KIDINS220	Kinase D-interacting substrate of 220 kDa	7.8	4
ACBD3 NS	+	38679884	SRI	Sorcin isoform b	7.8	3
ACBD3 CS	+	15826852	ACBD3	Golgi resident protein GCP60	23.5	842
ACBD3 CS	+	83641874	CPVL	Probable serine carboxypeptidase CPVL precursor	23.5	24
ACBD3 CS	+	149944715	PPM1H	Protein phosphatase 1H	23.5	16
ACBD3 CS	+	311771621	PI4KB	Phosphatidylinositol 4-kinase beta isoform 2	19.5	18
ACBD3 CS	+	154816184	TMEM55B	Transmembrane protein 55B isoform 2	19.5	11
ACBD3 CS	+	56549147	STEAP3	Metalloreductase STEAP3 isoform b	15.6	14
ACBD3 CS	+	4504805	BLZF1	Golgin-45	15.6	10
ACBD3 CS	+	38026892	ALG6	Dolichyl pyrophosphate Man9GlcNAc2 alpha-1,3- glucosyltransferase precursor	11.7	12
ACBD3 CS	+	22507409	TBC1D22A	TBC1 domain family member 22A	11.7	7
ACBD3 CS	+	19923748	DLST	Dihydrolipoyllysine residue succinyltransferase component of 2-oxoglutarate dehydrogenase complex, mitochondrial isoform 1 precursor	7.8	9
ACBD3 CS	+	34101272	BCKDHB	2-Oxoisovalerate dehydrogenase subunit beta, mitochondrial precursor	7.8	6
ACBD3 CS	+	40789249	DARS2	Aspartyl-tRNA synthetase, mitochondrial	7.8	3
ACBD3 CS	+	148839335	DPY19L1	Protein Dpy-19 homolog 1	7.8	2
ACBD3 CS	+	11559925	XPNPEP3	Probable Xaa–Pro aminopeptidase 3 isoform 1	7.8	2
TBC1D22A	−	22507409	TBC1D22A	TBC1 domain family member 22A	23.5	538
TBC1D22A	−	15826852	ACBD3	Golgi resident protein GCP60	23.5	42
TBC1D22A	−	4506583	RPA1	Replication protein A 70-kDa DNA binding subunit	11.7	36
TBC1D22A	−	4506587	RPA3	Replication protein A 14-kDa subunit	11.7	14
TBC1D22A	−	4506585	RPA2	Replication protein A 32-kDa subunit	11.7	6
TBC1D22A	−	17999541	VPS35	Vacuolar protein sorting- associated protein 35	7.8	10
TBC1D22A	−	124494254	PA2G4	Proliferation-associated protein 2G4	7.8	8
TBC1D22A	−	14211889	DPY30	Protein Dpy-30 homolog	7.8	6
TBC1D22A	−	17978519	VPS26A	Vacuolar protein sorting- associated protein 26A isoform 1	7.8	3
TBC1D22A	−	23397429	EIF3M	Eukaryotic translation initiation factor 3 subunit M	7.8	3
TBC1D22B	−	40068063	TBC1D22B	TBC1 domain family member 22B	23.5	1,575
TBC1D22B	−	15826852	ACBD3	Golgi resident protein GCP60	23.5	117
TBC1D22B	−	198041662	PYCRL	Pyrroline-5-carboxylate reductase 3	6.7	5
TBC1D22B	−	4505067	MAD2L1	Mitotic spindle assembly checkpoint protein MAD2A	6.7	5
TBC1D22B	−	150378533	USP7	Ubiquitin carboxyl-terminal hydrolase 7	6.7	4
TBC1D22B	−	51479145	ARFGEF1	Brefeldin A-inhibited guanine nucleotide exchange protein 1	6.7	4
PI4KB	−	311771621	PI4KB	Phosphatidylinositol 4-kinase beta isoform 2	23.5	1,686
PI4KB	−	15826852	ACBD3	Golgi resident protein GCP60	23.5	35
PI4KB	−	284807150	GBA	Glucosylceramidase isoform 2	18.8	23
PI4KB	−	294832006	PPP2R2A	Serine/threonine-protein phosphatase 2A 55-kDa regulatory subunit B alpha isoform 2	14.1	7
PI4KB	−	14141170	MTA2	Metastasis-associated protein MTA2	14.1	6
PI4KB	−	154350213	C10orf76	UPF0668 protein C10orf76	9.4	17
PI4KB	−	27363458	LRFN4	Leucine-rich repeat and fibronectin type III domain-containing protein 4 precursor	9.4	13

[a] Interacting proteins identified by AP-MS for ACBD3, TBC1D22A, TBC1D22B, and PI4KIIIb were weighted by *Z* score of the peptide counts. Proteins are listed here with replicate *Z* scores and peptide counts in the experimental set with a minimum of $n = 5$ biological replicates and were scored against a background set of 550 unrelated picornaviral protein AP-MS experiments, excluding the 3A protein itself (Materials and Methods). Shown here are the top-scoring proteins that appeared in at least two replicate experiments and with >1 count in at least one experiment; a full *Z* score table is provided in Table S1, Tab SI.4 in the supplemental material. The major interacting proteins for ACBD3 included TBC1D22A and PI4KB, as well as PPM1H, TMEM55B isoform 2, CPVL, and GOLGB1. Reciprocal AP-MS experiments with TBC1D22A, its closely related isoform TBC1D22B, and PI4KB confirmed interaction with ACBD3. Proteins are C-terminally StrepII-tagged (CS) unless otherwise noted as N-terminally tagged (NS).

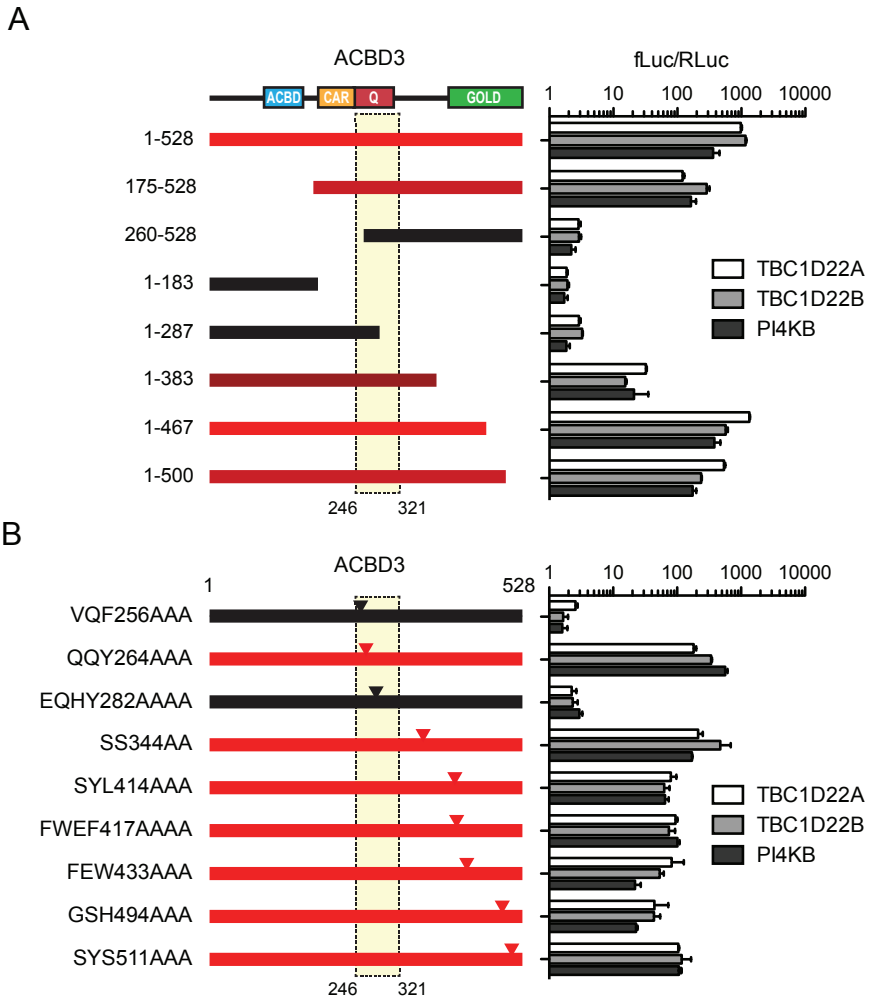

FIG 1 TBC1D22A/B interaction on ACBD3 is localized to the coiled-coil region and overlaps the PI4KB-interacting region. (A) Mapping of TBC1D22A/B and PI4KB binding localizes to the glutamine-rich (Q) region on ACBD3 by mammalian two-hybrid screening. The three proteins demonstrate similar binding values for all of the mutants tested, with a slight preference of TBC1D22A over TBC1D22B and PI4KB. (B) Alanine mutants across the C-terminal half of ACBD3 demonstrate that TBC1D22A/B and PI4KB binding to ACBD3 is disrupted only by mutations in the glutamine-rich region and not by mutations in the C-terminal GOLD domain. Binding values for the protein-protein interaction reporter (firefly luciferase) are plotted as a percentage of the transfection control values (*Renilla* luciferase). The graphical representation of each construct is colored based on the binding value. Low binding is depicted in black while high binding is depicted in red. The critical region defined by the collection of constructs is demarcated by the yellow box with the dashed outline (ACBD, acyl-CoA binding domain; CAR, charged amino acid region; Q, glutamine-rich region; GOLD, Golgi dynamics domain).

the role of the GOLD domain, as it appears to have an influence on the binding of these proteins as shown in Fig. 1A. We also note that TBC1D22A/B was not detected in any PI4KB AP-MS experiment nor was PI4KB detected in any TBC1D22A/B AP-MS experiment (see Table S1, Tab SI.3B–SI.3D). Together, these data support the notion that PI4KB and TBC1D22A/B participate in a mutually exclusive relationship with ACBD3.

The N terminus of TBC1D22A/B is required for ACBD3 interaction. To understand whether the RabGAP domain or some other region of TBC1D22A/B was responsible for the interaction with ACBD3, both mammalian two-hybrid mapping and AP-Western blotting were performed on deletion mutants of TBC1D22A/B. By both of these methods, the ACBD3-interacting region was localized to a predicted alpha-helix between residues 90 and 105 of TBC1D22A, demonstrating that the TBC domain was not required for binding (Fig. 2A; see also Fig. S4A in the supplemental material). Alanine scanning mutagenesis of this region revealed a valine-leucine residue pair that was required for ACBD3 binding along with a minor involvement of residues VVME93 (Fig. 2B; see also Fig. S4B).

TBC1D22A and TBC1D22B share 78% amino acid identity in their respective RabGAP domains yet share <40% amino acid identity outside the RabGAP domain. Deletion mapping of TBC1D22B similarly localized the ACBD3 interaction to a predicted alpha-helix with conserved sequence to TBC1D22A, including the valine-leucine pair (Fig. 2C; see also Fig. S4C in the supplemental material). Alanine scanning of this region on TBC1D22B also revealed substantial defects (≥100-fold decrease) in binding, especially at VL100 (Fig. 2D). Mutation of phosphorylation sites on TBC1D22B discovered by mass spectrometry, all of which reside outside the identified interacting region, to glutamic acid as a phosphomimetic did not affect binding to ACBD3 (see Fig. S4D and Table S1, Tab SI.6). Mammalian two-hybrid mapping on TBC1D22A/B was confirmed by AP-Western blotting and AP-MS (see Fig. S4A to C). Interestingly, six total AP-MS experiments with full-length TBC1D22A and TBC1D22B and deletion mutants of TBC1D22A, all of which retained ACBD3 binding, showed that they copurified with ARFGEF1, a trans-Golgi membrane-localized Sec7 domain containing the guanine exchange factor for Arf1 (14). This interaction is highly specific, as peptides to ARFGEF1 were detected in only those six deletion and full-length TBC1D22A/B AP-MS experiments out of a total of >2,100 AP-MS runs in our lab (spectra are provided in Fig. S1).

Deletion mapping, alanine mutagenesis, and AP-Western blotting of TBC1D22A revealed a significant involvement of serines 165 and 167 for 14-3-3 protein recruitment. This site matches the canonical type I 14-3-3 binding motif of R-[SFYW]-X-pS-X-P, suggesting that serine 167 is the phosphorylated serine responsible for 14-3-3 recruitment (15). TBC1D22A deletion and point mutants that disrupted 14-3-3 binding retained the ability to bind ACBD3, while the TBC1D22A VL101AA mutant that disrupted ACBD3 interaction was still able to bind 14-3-3 isoforms, similarly to wild-type TBC1D22A (Fig. 2A; see also Fig. S4B in the supplemental material). While the significance of TBC1D22A in-

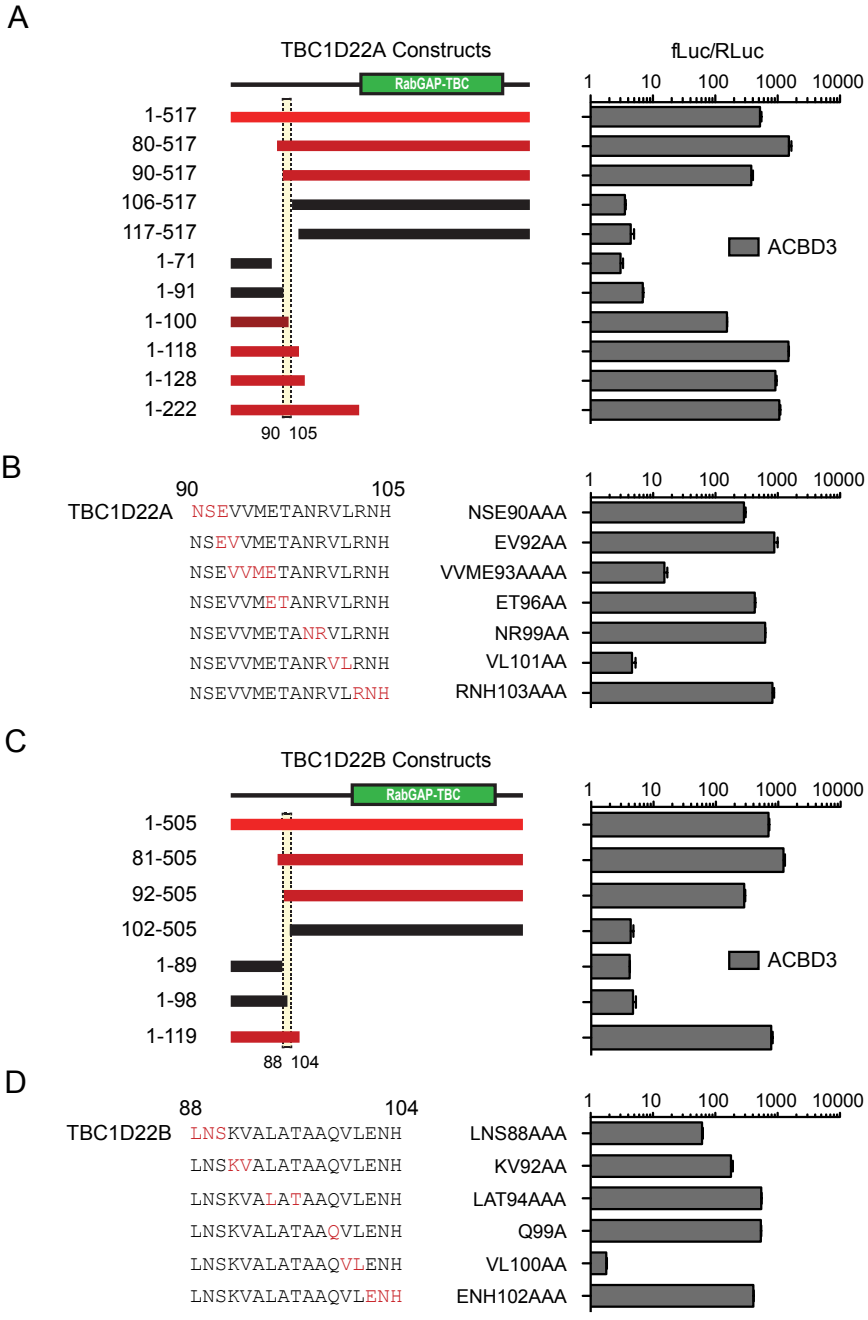

FIG 2 ACBD3 interaction localizes to the N terminus on TBC1D22A and TBC1D22B and is disrupted by the same valine-leucine mutation. (A) Deletion mutagenesis of TBC1D22A specifically localizes its interaction with ACBD3 by mammalian 2-hybrid screening to a predicted N-terminal helix near residues 90 to 105. (B) Alanine scanning reveals a critical dependence on residues VL101 with a contribution from VVME93. (C) Deletion mutagenesis of TBC1D22B also localizes its interaction with ACBD3 to a predicted N-terminal helix, as in TBC1D22A, despite an amino acid identity of <40% outside the RabGAP domain. (D) Alanine scanning across the TBC1D22B helix demonstrates that the ACBD3 interaction is significantly disrupted by the VL100AA mutation, as well as a contribution from upstream residues LNS88.

teraction with 14-3-3 proteins remains unknown, these data suggest that TBC1D22A interaction with ACBD3 is not mediated by 14-3-3 isoforms or vice versa.

PI4KB-ACBD3 interaction maps to the N terminus of PI4KB. We employed both AP-Western blotting and mammalian two-hybrid mapping in conjunction with deletion mutants to localize the region of PI4KB required for interaction with ACBD3 (Fig. 3). By N-terminal and C-terminal deletion, a region of 19 amino acids, extending from residues 53 to 70, of PI4KB was necessary for interaction with ACBD3 by both assays, indicating that the catalytic domain, the lipid kinase unique (LKU) region, and the Hom2 region of PI4KB were dispensable (16) (Fig. 3A; see also Fig. S5A, B, and C in the supplemental material). Analogously to what was found in TBC1D22A/B, alanine scanning of this narrow region in PI4KB revealed that a valine-leucine pair (VL67) was required for ACBD3 interaction with additional contribution from upstream residues (Fig. 3B), suggesting that these two proteins bind ACBD3 via similar motifs. These results were also confirmed by AP-Western blotting (see Fig. S5A to C). Two mutants, VL67 and IDP55, that retained the ability to bind alternative PI4KB partners, C10orf76 and Rab11B, were identified, suggesting that the ACBD3 binding deficit was specific (Fig. 3B). We note that the QE65AA mutant demonstrated no ability to bind C10orf76 or Rab11B but bound to ACBD3 at levels 6-fold greater than those for the wild type according to the mammalian two-hybrid reporter (Fig. 3B), although it is not necessarily clear whether these differences in binding are due to increased binding to one factor or to an inability to bind another competing factor. Finally, mutation of PI4KB phosphorylation sites discovered by mass spectrometry, all of which reside outside the critical interaction region, to glutamic acid did not affect binding to ACBD3, C10orf76, or Rab11B (see Fig. S5D).

TBC1D22A/B competes with PI4KB for ACBD3 binding *in vitro*. The combined AP-MS and fine-scale mapping data for TBC1D22A/B and PI4KB suggest a mutually exclusive binding relationship with ACBD3. If this were the case, we would expect there to be a competitive binding relationship between these two proteins and ACBD3. To qualitatively test this hypothesis in a competition experiment, increasing amounts of protein lysate from 293T cells expressing TBC1D22A-Flag were added to premixed 293 lysate from PI4KB-V5- and ACBD3-Strep-expressing cells (Fig. 4A). Affinity purification of ACBD3-Strep revealed decreasing amounts of copurified PI4KB-V5 as a function of increasing amounts of TBC1D22A-Flag (Fig. 4B). This competition was independent of RabGAP activity, as only the N terminus of

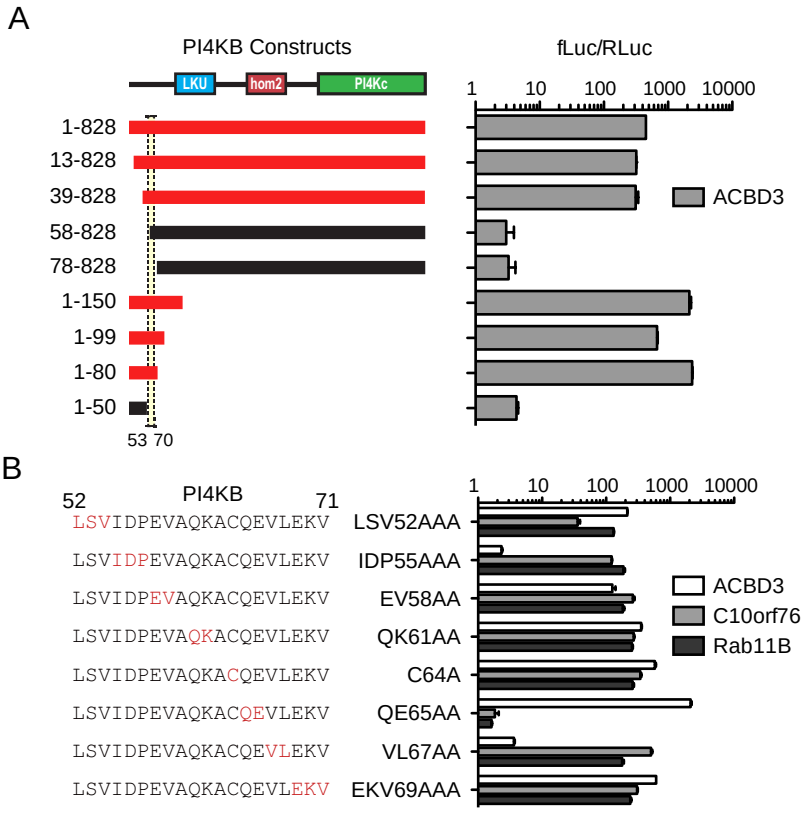

FIG 3 ACBD3 interaction localizes to the N terminus on PI4KB and is disrupted by the same valine-leucine mutation. (A) Deletion mapping of PI4KB localizes its interaction with ACBD3 to the far N terminus on PI4KB by mammalian 2-hybrid screening. (B) Alanine scanning of the putative alpha-helix on PI4KB demonstrated a significant contribution of residues VL67 and IDP55 to its interaction with ACBD3. Binding of PI4KB interactors Rab11B and C10orf76 was used to control for global protein defects. Mutant QE65AA abrogated binding of PI4KB to C10orf76 and Rab11B but increased binding to ACBD3 by 6-fold.

TBC1D22A was required (Fig. 4C). 293T cell lysate that did not express TBC1D22A-Flag could not compete off PI4KB-V5 (Fig. 4D).

3A binding region of ACBD3 localizes to the GOLD domain and associates with ACBD3 self-binding. Previously, we and others demonstrated that enteroviral and kobuviral 3A proteins interact with ACBD3 by AP-MS and AP-Western blotting (5, 6). To test whether other picornavirus 3A proteins bound ACBD3 more transiently, we tested hepatovirus, klassevirus, parechovirus, cardiovirus, and aphthovirus 3A proteins in the mammalian two-hybrid assay. In this assay, both kobuvirus and enterovirus 3A proteins bound most strongly to ACBD3 while the 3A proteins of hepatovirus, klassevirus, and parechovirus all demonstrated a significant but lesser (approximately 10-fold) ability to bind ACBD3 (Fig. 5A). Cardiovirus and aphthovirus 3A proteins did not demonstrate binding to ACBD3 above background.

Aichi virus 3A interaction with ACBD3 was previously mapped to the GOLD domain of ACBD3 (6). Given the broad range of picornavirus 3A proteins interacting with ACBD3, we used the mammalian two-hybrid reporter system to investigate whether these 3A proteins also interacted with the C-terminal GOLD domain. Both poliovirus and Aichi virus 3A proteins mapped to the C-terminal half of ACBD3 (Fig. 5B), consistent with deletion mapping by AP-Western blotting. To further refine the deletion mapping, we found that alanine mutations in the coiled-coil region of ACBD3 that did not bind TBC1D22A/B and PI4KB (VQF255AAA and EQHY281AAAA) retained picornavirus 3A binding. However, all alanine mutations in the GOLD domain disrupted binding of both picornaviral 3A proteins (Fig. 5C). One mutation near the C terminus (SYS511AAA or Y512A) demonstrated a slight difference in preference of poliovirus 3A over Aichi virus 3A, suggesting that the binding between the two proteins may be only subtly different (Fig. 5C; see also Fig. S3B in the supplemental material).

Fine-scale mapping indicated that binding of the 3A proteins was critically dependent on the presence of Tyr residue 525, only three amino acids from the C-terminus of wild-type ACBD3 (Fig. 5D). Mapping of the hepatitis A virus (HAV) and klassevirus 3A interactions with ACBD3 revealed an interaction profile similar to those of Aichi virus and poliovirus 3A (see Fig. S6 in the supplemental material), suggesting that these diverse picornaviruses bind ACBD3 in an analogous manner despite their wide sequence divergence (17–19).

The critical dependence of multiple GOLD domain-interacting proteins on the presence of Tyr-525 for binding to ACBD3 suggested that a potential intramolecular ACBD3 interaction was required. We tested whether ACBD3 could bind itself in the context of the mammalian two-hybrid assay. ACBD3 demonstrated an interaction with itself that mapped to GOLD domain as well as the threshold effect at Tyr-525 (Fig. 5B to D). Mutations in GOLD domain that disrupted interaction with ACBD3-interacting partners similarly disrupted ACBD3 homomerization. However, one mutant (SYL414AAA) specifically disrupted ACBD3 homomerization while only slightly decreasing binding to poliovirus 3A and Aichi virus 3A, demonstrating that 3A binding to ACBD3 is not dependent on ACBD3 homomerization, at least for these viral species, as klassevirus 3A and hepatitis A virus 3A did not bind the ACBD3 SYL414AAA mutant above background (see Fig. S6B in the supplemental material). While these results are suggestive of a possible interplay between ACBD3 homomerization and binding by viral 3A proteins, additional biochemical characterization will be required to explore this dynamic.

ACBD3 binding regions on picornavirus 3A are distinct. To further investigate the possibility of differential ACBD3 interactions with Aichi virus and poliovirus 3A proteins, we extended our deletion and mammalian two-hybrid mapping of the ACBD3-interacting region for both of these proteins. Deletion of the C-terminal half of poliovirus 3A reduced ACBD3 binding by 100-fold, while a comparable deletion in Aichi virus 3A retained ACBD3 binding (Fig. 6A and B), consistent with previous results in which alanine scanning the entirety of Aichi virus 3A revealed only two point mutations that affected ACBD3 binding (5). N-terminal deletions in the GBF1 binding domain of poliovirus 3A significantly increased ACBD3 binding relative to that of the wild type by more than 10-fold (Fig. 6A). Alanine scanning of

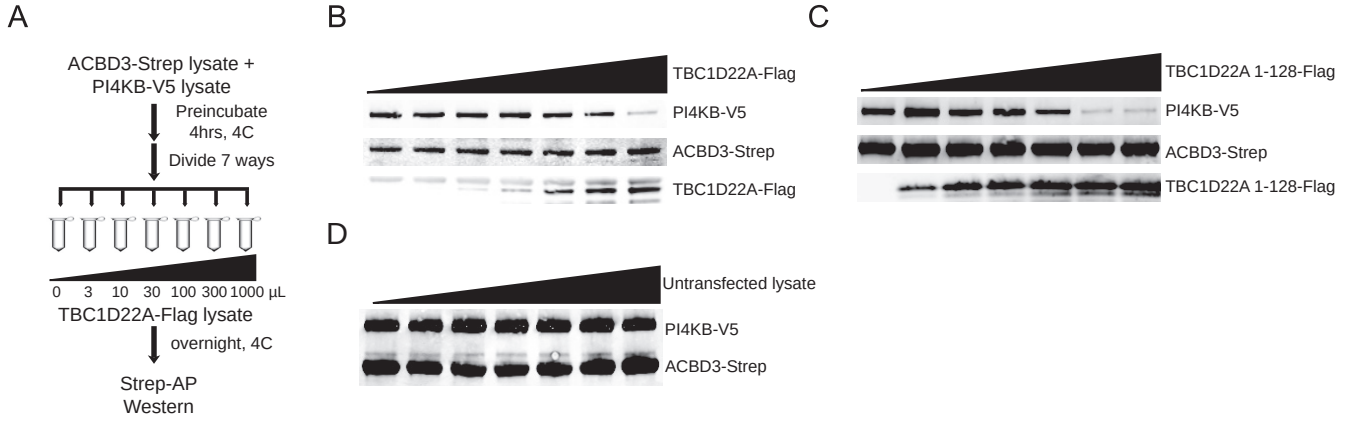

FIG 4 The N terminus of TBC1D22A can compete with PI4KB for binding of ACBD3. (A) Experimental setup to test for binding competition. V5-tagged PI4KB expressing 293T lysate was premixed with Strep-tagged ACBD3 expressing 293T lysate and divided seven ways. Increasing amounts of Flag-tagged TBC1D22A expressing 293T lysate were added to each tube, and lysates were affinity purified for Strep-tagged ACBD3 and assayed by Western blotting with anti-V5, anti-Strep, and anti-Flag antibodies. (B) Addition of increasing amounts of full-length TBC1D22A-Flag reduces the amount of PI4KB-V5 bound by ACBD3-Strep. (C) A Flag-tagged N-terminal fragment (1 to 128) of TBC1D22A is sufficient to compete off PI4KB-V5 from ACBD3-Strep. (D) Untransfected lysate is unable to compete PI4KB-V5 from ACBD3-Strep.

much of the N-terminal half of poliovirus 3A revealed several point mutants C terminal to the GBF1 binding site that were critical for binding ACBD3 by AP-Western blotting (D29A, R34A, KKGW42-KGA, and R54A) (see Fig. S9C in the supplemental material). These results implicate multiple portions of Aichi virus 3A for binding to ACBD3, while poliovirus 3A appears to contain a defined ACBD3 binding domain that is C-terminal to its GBF1 binding region and dimerization region (20).

Kobuviral 3A proteins prevent TBC1D22A binding to ACBD3, while enterovirus 3A proteins do not. Given that TBC1D22A/B appears to compete with PI4KB for ACBD3 binding and that picornaviruses are dependent on PI4KB for activity, we hypothesized that picornavirus 3A interaction with ACBD3 could influence the outcome of this competition. We note that in the picornavirus 3A AP-MS data that we have published previously (5), peptides to TBC1D22A/B were recovered in multiple enteroviral 3A AP-MS experiments while no peptides to TBC1D22A/B were ever identified in kobuviral 3A AP-MS experiments where a stable ACBD3-PI4KB complex was identified (see Table S1, Tab SI.4 in the supplemental material) (5). To test this hypothesis, we examined whether the presence of different 3A proteins affected the TBC1D22A-ACBD3 interaction. We coexpressed kobuvirus 3A and enterovirus 3A proteins together with TBC1D22A and then assayed affinity-purified TBC1D22A by Western blotting. Whereas the expression of enterovirus 3A proteins did not affect the recovery of affinity-purified TBC1D22A, we observed an apparent affect on the expression of TBC1D22A in the presence of kobuvirus 3A (see Fig. S7).

We investigated whether the presence of Aichi virus 3A or poliovirus 3A could affect the endogenous level of TBC1D22A mRNA. Using HEK293T cells transfected with Aichi virus 3A-Flag or poliovirus 3A-Flag, we measured the level of TBC1D22A mRNA by quantitative reverse transcription-PCR (qRT-PCR). There was no significant difference in the level of TBC1D22A mRNA in the presence of poliovirus 3A and only modest changes ($<$14%) in the presence of TBC1D22A (see Fig. S8 in the supplemental material).

To investigate the effect of picornavirus 3A protein interaction with respect to PI4KB and TBC1D22A interaction with ACBD3, and to avoid the apparent effect of coexpression differences in the presence of 3A proteins, we separated the expression of the proteins by independently transfecting Flag-tagged picornavirus 3A proteins and TBC1D22A-V5 into different plates of HEK293T cells. We then immunoprecipitated TBC1D22A-V5 complexes onto beads and added exogenous HEK293T lysates containing overexpressed poliovirus 3A-Flag and Aichi virus 3A-Flag. Finally, the TBC1D22A-V5 beads were recovered and assayed for ACBD3 and 3A-Flag recruitment by Western blotting (Fig. 7A). Poliovirus 3A-Flag could be readily detected in TBC1D22A-ACBD3-containing complexes, while Aichi virus 3A-Flag could not (Fig. 7B). Quantification of this difference demonstrated a $>$7-fold increase in poliovirus 3A recovery from the TBC1D22A-V5 beads over that of Aichi virus 3A (Fig. 7C). Collectively, these results support a model whereby the kobuviral and enteroviral 3A proteins may differentially modulate the interaction of PI4KB and TBC1D22A/B with ACBD3.

DISCUSSION

In this study, we have identified TBC1D22A/B as a new interacting partner of ACBD3, a protein of central importance in Golgi organization and picornaviral replication. TBC1D22A/B is a Golgi membrane-localized putative Rab33 RabGAP (9). Altered ER-Golgi morphology has been associated with overexpression of TBC1D22B and is dependent on the presence of TBC1D22B RabGAP activity (10). We found that the interaction between TBC1D22A/B and ACBD3 was dependent on a narrow region that maps to a predicted helix in the N terminus of TBC1D22A/B. This interaction may determine localization of these RabGAPs to the Golgi membrane and their ability to affect Golgi morphology. TBC1D22A/B bound to the same region on ACBD3 as did PI4KB, and we found that the same residues that were critical for TBC1D22A/B binding were also critical for PI4KB binding. Together with our finding that TBC1D22A/B directly competed with PI4KB for ACBD3 binding, this suggests that, in addition to putatively regulating Rab33 GTP binding at the Golgi membrane, these RabGAPs may in part determine the Golgi membrane local-

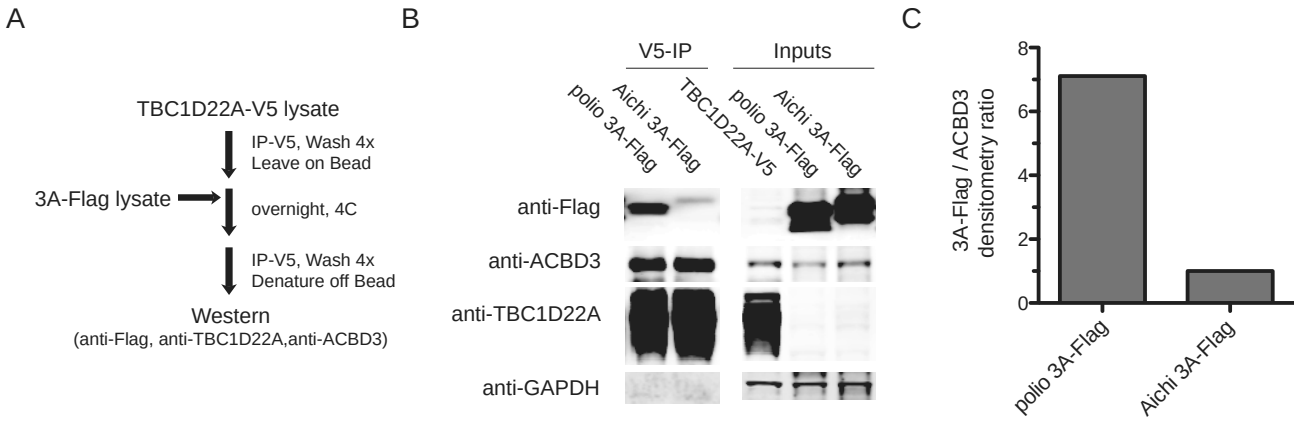

FIG 7 Aichi virus 3A does not occupy the same ACBD3 as does TBC1D22A, while poliovirus 3A proteins can occupy the same ACBD3 as does TBC1D22A. (A) Experimental setup to test the influence of 3A proteins on the interaction of TBC1D22A with ACBD3. V5-tagged TBC1D22A, Flag-tagged Aichi virus 3A, and Flag-tagged poliovirus 3A were each singly transfected into a 15-cm plate of HEK293T cells. TBC1D22A-V5 was immunoprecipitated with anti-V5 beads, washed 4 times, and left on the bead, to which Flag-tagged picornaviral 3A protein lysate was added and left to incubate overnight at 4°C. This lysate was again centrifuged with the anti-V5 beads and washed 4 times, and then captured proteins were boiled off the beads in SDS sample buffer to examine whether 3A-Flag could occupy the same ACBD3 as TBC1D22A by Western blotting. (B) Flag-tagged Aichi virus 3A does not copurify with TBC1D22A-V5 and bound ACBD3, while Flag-tagged poliovirus 3A copurifies with TBC1D22A-V5 and its captured ACBD3 by Western blotting. (C) Quantification of bound poliovirus 3A-Flag relative to Aichi virus-Flag, adjusted for the amount of ACBD3 pulled down, reveals a 7-fold difference in binding.

interaction with ACBD3 without phosphorylation (15). At present, in the absence of three-dimensional structure information for each of these proteins, it is not clear what regulates the binding of TBC1D22A/B versus PI4KB to the glutamine-rich region of ACBD3.

The picornaviral 3A proteins may inform the cellular biology that regulates whether TBC1D22A/B or PI4KB is bound to ACBD3. An open question in picornavirus biology is why enteroviruses retain a specific GBF1 recruitment domain and are sensitive to brefeldin A while kobuviruses do not bind GBF1 and are insensitive to brefeldin A. Given that multiple picornaviruses rely on ACBD3 and PI4KB, direct competition by TBC1D22A/B suggests that viruses have evolved a mechanism to subvert cellular regulation of these two proteins. Our data show that the kobuviral 3A proteins appear to abrogate the binding of TBC1D22A/B to ACBD3, thus favoring the formation of a stable 3A-ACBD3-PI4KB complex that remains even after 25 to 30 min of washing. This stable complex may obviate the need for GBF1 recruitment and activity and allow kobuviruses to directly influence PI4KB localization and activity with respect to viral replication in a manner similar to, yet distinct from, that of enterovirus 3A. It is also remarkable that a protein that binds entirely to the GOLD domain can manipulate the binding of proteins in other domains of ACBD3, suggesting cross talk between ACBD3's various domains. Although we have mapped the critical binding region of TBC1D22A/B to the Q-rich region of ACBD3, we cannot discount the role of the GOLD domain, as it appears to have an influence on the binding of these proteins as shown in Fig. 1A.

It is not clear if or how enteroviruses manipulate the TBC1D22A/B-ACBD3 interaction, given that enterovirus 3A and TBC1D22A/B appear to occupy the same ACBD3 in our affinity purifications. The ACBD3-PI4KB-TBC1D22A/B system may provide a clue as to why enterovirus 3A proteins directly bind to and require GBF1 for replication. Mapping of the ACBD3-interacting region on the poliovirus 3A protein demonstrated an ACBD3 binding domain C-terminal to the region responsible for binding GBF1, suggesting that poliovirus 3A's recruitment of GBF1 to Golgi membranes might be for recruitment of GBF1 to ACBD3. GBF1-Arf1 dynamics at the membrane may be responsible for recruiting another regulator that determines whether TBC1D22A/B or PI4KB is bound to ACBD3. Our affinity purification conditions may not promote the formation of a 3A-GBF1-ACBD3-PI4KB complex, thus allowing TBC1D22A/B to compete off PI4KB from ACBD3.

The reliance on overexpressed proteins in these protein-protein interaction studies is an important caveat. For example, nonphysiological levels of ACBD3 and/or TBC1D22A/B could produce an interaction that would be unlikely to occur at native levels. While our attempts to address this have been hampered by the lack of immunoprecipitation-competent antibodies to the untagged version of TBC1D22A/B, we have previously published experiments which indicate that ACBD3 and TBC1D22A/B interact at native expression levels. Specifically, we note that native TBC1D22A/B copurified with native ACBD3 in the presence of affinity-purified enterovirus 3A proteins, suggesting that the interaction is not entirely an artifact of overexpressing ACBD3 or TBC1D22A/B (see Table S7 in reference 5).

Future experiments with the PI4KB mutants isolated in this study will help illuminate whether different PI4KB mutants can rescue enterovirus replication after depletion of native PI4KB. However, it is of note that enteroviruses selected for resistance to enviroxime family PI4KB inhibitors contain mutations in the ACBD3 binding region of 3A (V45A and H57Y) (25). How these mutants affect ACBD3 binding by 3A and whether PI4KB can compete TBC1D22A/B off ACBD3 are important outstanding questions.

In conclusion, multiple picornaviruses coopt the same central ACBD3-PI4KB axis for replication but utilize different cellular mechanisms to manipulate the system. The kobuviruses and enteroviruses may reflect convergent evolutionary strategies to manipulate this key lipid regulator. The mutants obtained in this study will be useful tools to test whether PI4KB localization to ACBD3 is required for picornavirus replication; to test the effect

of ACBD3, TBC1D22A/B, and GBF1 on PI4P levels in the cell; and to discover regulatory mechanisms that govern the ACBD3 interactome.

MATERIALS AND METHODS

Cells, plasmids, and cloning. 293T cells were maintained in Dulbecco modified Eagle medium (DMEM)-H21 medium supplemented with 10% fetal bovine serum (FBS) and penicillin-streptomycin. All genes for transient transfections were cloned into a modified pCDNA4-TO vector containing an N-terminal or C-terminal 2× Strep II-tag as described previously using primers from Table S1 in the supplemental material (26). Accession numbers used for genes were as follows: ACBD3, NM_0022735; PI4KB, NM_002651; TBC1D22A, NM_014346; TBC1D22B, NM_017772; Rab11B. The human C10orf76 gene was synthesized commercially (BioBasic Inc., Canada).

Transient transfections were performed in a 15-cm plate of 293T cells at 50 to 60% confluency using 10 μg of total plasmid and a 3:1 ratio of TransIT-LT1 transfection reagent to plasmid (Mirus Bio). Protein lysates were prepared in 0.5% NP-40 in a background buffer of either 50 mM Tris-HCl (pH 8.0), 150 mM NaCl, 1 mM EDTA or 50 mM HEPES-KOH (pH 6.8), 150 mM potassium acetate (KOAc), 2 mM magnesium acetate (MgOAc), 1 mM $CaCl_2$, 15% glycerol, 1× Roche EDTA-free protease inhibitor cocktail. Affinity purifications and Western blotting assays were otherwise performed as described previously (5, 26).

For the ACBD3 binding competition assay, transient transfections of ACBD3-Strep, TBC1D22A-Flag, and PI4KB-V5 in individual 15-cm plates of 293T cells were performed as described above. Lysates from each plate were prepared in 2 ml of EDTA-containing buffer. PI4KB-V5 and ACBD3-Strep lysate were premixed in a 15-ml Falcon tube for 4 h at 4°C. The lysate was then divided into 7 aliquots of 500 μl each, and 0, 3, 10, 30, 100, 300, and 1,000 μl of lysate from the TBC1D22A-Flag-transfected plate or an untransfected plate was added to the aliquots along with 35 μl of StrepTactin resin (IBA Life Sciences) and incubated overnight at 4°C. ACBD3-Strep was affinity purified, and copurified TBC1D22A-Flag and PI4KB-V5 were detected by Western staining using anti-Flag and anti-V5 antibodies (Sigma). For the 3A-TBC1D22A cotransfection experiments (see Fig. S8 in the supplemental material), 2.5 μg of TBC1D22A-Strep and 7.5 μg of picornavirus 3A-Flag were cotransfected using Mirus TransIT-LT1 transfection reagent as described above.

Mammalian two-hybrid screening. Interaction mapping was performed by mammalian two-hybrid screening using the Checkmate system (Promega, Madison, WI). Bait proteins were cloned into the pAct and pBind plasmids using the KpnI and EcoRV restriction sites and primers as described in Table S1 in the supplemental material. Thirty-three nanograms each of pAct, pBind, and pG5Luc plasmids was transfected into 15,000 293T cells plated 24 h previously in each well of a 96-well plate. Firefly and *Renilla* luciferase levels were measured using the dual-luciferase assay kit 40 to 48 h after transfection (Promega). The level of binding is expressed as firefly luciferase values as a percentage of transfection control *Renilla* luciferase values, measured on a Veritas microplate luminometer.

qRT-PCR. For qRT-PCR, 1 μg of Aichi virus 3A-Flag or poliovirus 3A-Flag was transfected into a 6-well plate of HEK293T cells in log phase and harvested 48 h later. Total RNA was extracted using the RNeasy kit (Qiagen). Two micrograms of total RNA from HEK293T cells was reverse transcribed using SuperScript III reverse transcriptase and oligo$(dT)_{20}$, and qRT-PCR was performed using the 480 DNA SYBR Green I master mix (Roche) on a LightCycler (Roche). Primers used were the TBC1D22A-CDS4 and hRPL19 set at a melting temperature (T_m) of 50°C and with an extension of 1 min at 72°C (see Table S1 in the supplemental material).

Protein identification by mass spectrometry. Protein identification from affinity-purified samples was performed using peptide sequencing by mass spectrometry as previously reported (5). Affinity-purified samples were reduced and alkylated with dithiothreitol (DTT) and iodoacetamide, respectively, and then subjected to trypsin digestion either in solution or in excised SDS-PAGE gel bands. Peptide sequencing was performed using an LTQ-FT, an LTQ-Orbitrap XL, or an LTQ-Velos (Thermo) mass spectrometer, each equipped with 10,000-psi system nanoACUITY (Waters) ultra-high-performance liquid chromatography (UPLC) instruments for reversed-phase C_{18} chromatography and using the same data acquisition and processing methods as those previously reported (5).

Database searches were performed against the *Homo sapiens* plus *Virus* subset of the NCBInr RefSeq database (14 January 2012), to which were added virus clone sequences missing from the public database, totaling 131,457 entries. This database was concatenated with a fully randomized set of 131,457 entries for estimation of the false discovery rate (27). Data were searched with a parent mass tolerance of 20 ppm and fragment mass tolerances of 0.6 Da.

Using peptide counts as an approximation of protein abundance, *Z* scores were calculated to represent prey-bait specificity as reported previously (5). *Z* scores for proteins interacting with individual virus or human bait proteins were calculated using a minimum of five replicate experiments together with a background model of 550 control, nonhuman bait data sets. These nonhuman data sets were compiled from the genes from 12 different picornaviruses, excluding the 3A gene itself (VP0/VP2, VP4, VP1, VP3, L, 2A, 2B, 2C, 3C, and 3D), which serve as an unbiased set of proteins that should be orthogonal to the human protein-protein interactions in this network. The nonspecific interacting proteins most commonly identified in this background set, analogous to "frequent fliers" reported as common contaminants in Flag-AP-MS experiments, are reported in Table S2 in the supplemental material (28).

SUPPLEMENTAL MATERIAL

Supplemental material for this article may be found at http://mbio.asm.org/lookup/suppl/doi:10.1128/mBio.00098-13/-/DCSupplemental.

Figure S1, PDF file, 0.3 MB.
Figure S2, PDF file, 1.2 MB.
Figure S3, PDF file, 0.1 MB.
Figure S4, PDF file, 1.3 MB.
Figure S5, PDF file, 1.7 MB.
Figure S6, PDF file, 0.1 MB.
Figure S7, PDF file, 1.1 MB.
Figure S8, PDF file, 1 MB.
Figure S9, PDF file, 0.9 MB.
Table S1, XLSX file, 0.4 MB.
Text S1, DOC file, 0.1 MB.

ACKNOWLEDGMENTS

Mass spectrometry analysis was performed in the Bio-Organic Biomedical Mass Spectrometry Resource at UCSF (A. L. Burlingame, director) supported by the Biomedical Technology Research Programs of the NIH (NIGMS), NIH 8P41GM103481, and the Howard Hughes Medical Institute. J.L.D. is supported by the Howard Hughes Medical Institute.

We also thank Christopher Nelson and Stephanie Moquin for careful reading of the manuscript.

REFERENCES

1. **Miller S, Krijnse-Locker J.** 2008. Modification of intracellular membrane structures for virus replication. Nat. Rev. Microbiol. **6**:363–374.
2. **Belov GA, Feng Q, Nikovics K, Jackson CL, Ehrenfeld E.** 2008. A critical role of a cellular membrane traffic protein in poliovirus RNA replication. PLoS Pathog. **4**:e1000216. http://dx.doi.org/10.1371/journal.ppat.1000216.
3. **Hsu NY, Ilnytska O, Belov G, Santiana M, Chen YH, Takvorian PM, Pau C, van der Schaar H, Kaushik-Basu N, Balla T, Cameron CE, Ehrenfeld E, van Kuppeveld FJM, Altan-Bonnet N.** 2010. Viral reorganization of the secretory pathway generates distinct organelles for RNA replication. Cell **141**:799–811.
4. **Belov GA, Kovtunovych G, Jackson CL, Ehrenfeld E.** 2010. Poliovirus replication requires the N terminus but not the catalytic Sec7 domain of ArfGEF GBF1. Cell. Microbiol. **12**:1463–1479.

5. **Greninger AL, Knudsen GM, Betegon M, Burlingame AL, Derisi JL.** 2012. The 3A protein from multiple picornaviruses utilizes the Golgi adaptor protein ACBD3 to recruit PI4KIIIβ. J. Virol. **86**:3605–3616.
6. **Sasaki J, Ishikawa K, Arita M, Taniguchi K.** 2012. ACBD3-mediated recruitment of PI4KB to picornavirus RNA replication sites. EMBO J. **31**:754–766.
7. **Sohda M, Misumi Y, Yamamoto A, Yano A, Nakamura N, Ikehara Y.** 2001. Identification and characterization of a novel Golgi protein, GCP60, that interacts with the integral membrane protein giantin. J. Biol. Chem. **276**:45298–45306.
8. **Rönnberg T, Jääskeläinen K, Blot G, Parviainen V, Vaheri A, Renkonen R, Bouloy M, Plyusnin A.** 2012. Searching for cellular partners of hantaviral nonstructural protein NSs: Y2H screening of mouse cDNA library and analysis of cellular interactome. PLoS One **7**:e34307. http://dx.doi.org/10.1371/journal.pone.0034307.
9. **Pan X, Eathiraj S, Munson M, Lambright DG.** 2006. TBC-domain GAPs for Rab GTPases accelerate GTP hydrolysis by a dual-finger mechanism. Nature **442**:303–306.
10. **Haas AK, Yoshimura S, Stephens DJ, Preisinger C, Fuchs E, Barr FA.** 2007. Analysis of GTPase-activating proteins: Rab1 and Rab43 are key Rabs required to maintain a functional Golgi complex in human cells. J. Cell Sci. **120**:2997–3010.
11. **Obsilová V, Silhan J, Boura E, Teisinger J, Obsil T.** 2008. 14-3-3 proteins: a family of versatile molecular regulators. Physiol. Res. **57**(Suppl 3):S11–S21.
12. **Hausser A, Link G, Hoene M, Russo C, Selchow O, Pfizenmaier K.** 2006. Phospho-specific binding of 14-3-3 proteins to phosphatidylinositol 4-kinase III β protects from dephosphorylation and stabilizes lipid kinase activity. J. Cell Sci. **119**:3613–3621.
13. **Jovic M, Kean MJ, Szentpetery Z, Polevoy G, Gingras AC, Brill JA, Balla T.** 2012. Two phosphatidylinositol 4-kinases control lysosomal delivery of the Gaucher disease enzyme, β-glucocerebrosidase. Mol. Biol. Cell **23**:1533–1545.
14. **Manolea F, Claude A, Chun J, Rosas J, Melançon P.** 2008. Distinct functions for arf guanine nucleotide exchange factors at the Golgi complex: GBF1 and BIGs are required for assembly and maintenance of the Golgi stack and trans-Golgi network, respectively. Mol. Biol. Cell **19**:523–535.
15. **Johnson C, Crowther S, Stafford MJ, Campbell DG, Toth R, MacKintosh C.** 2010. Bioinformatic and experimental survey of 14-3-3-binding sites. Biochem. J. **427**:69–78.
16. **Altan-Bonnet N, Balla T.** 2012. Phosphatidylinositol 4-kinases: hostages harnessed to build panviral replication platforms. Trends Biochem. Sci. **37**:293–302.
17. **Greninger AL, Runckel C, Chiu CY, Haggerty T, Parsonnet J, Ganem D, DeRisi JL.** 2009. The complete genome of klassevirus—a novel picornavirus in pediatric stool. Virol. J. **6**:82. http://dx.doi.org/10.1186/1743-422X-6-82.
18. **Holtz LR, Finkbeiner SR, Zhao G, Kirkwood CD, Girones R, Pipas JM, Wang D.** 2009. Klassevirus 1, a previously undescribed member of the family Picornaviridae, is globally widespread. Virol. J. **6**:86. http://dx.doi.org/10.1186/1743-422X-6-86.
19. **Li L, Victoria J, Kapoor A, Blinkova O, Wang C, Babrzadeh F, Mason CJ, Pandey P, Triki H, Bahri O, Oderinde BS, Baba MM, Bukbuk DN, Besser JM, Bartkus JM, Delwart EL.** 2009. A novel picornavirus associated with gastroenteritis. J. Virol. **83**:12002–12006.
20. **Wessels E, Duijsings D, Lanke KHW, Melchers WJG, Jackson CL, van Kuppeveld FJM.** 2007. Molecular determinants of the interaction between coxsackievirus protein 3A and guanine nucleotide exchange factor GBF1. J. Virol. **81**:5238–5245.
21. **Dong N, Zhu Y, Lu Q, Hu L, Zheng Y, Shao F.** 2012. Structurally distinct bacterial TBC-like GAPs link Arf GTPase to Rab1 inactivation to counteract host defenses. Cell **150**:1029–1041.
22. **Neunuebel MR, Machner MP.** 2012. The taming of a Rab GTPase by Legionella pneumophila. Small GTPases **3**:28–33.
23. **Nevo-Yassaf I, Yaffe Y, Asher M, Ravid O, Eizenberg S, Henis YI, Nahmias Y, Hirschberg K, Sklan EH.** 2012. Role for TBC1D20 and Rab1 in hepatitis C virus replication via interaction with lipid droplet-bound nonstructural protein 5A. J. Virol. **86**:6491–6502.
24. **Sklan EH, Serrano RL, Einav S, Pfeffer SR, Lambright DG, Glenn JS.** 2007. TBC1D20 is a Rab1 GTPase-activating protein that mediates hepatitis C virus replication. J. Biol. Chem. **282**:36354–36361.
25. **Van der Schaar HM, van der Linden L, Lanke KHW, Strating JRPM, Pürstinger G, de Vries E, de Haan CAM, Neyts J, van Kuppeveld FJM.** 2012. Coxsackievirus mutants that can bypass host factor PI4KIIIβ and the need for high levels of PI4P lipids for replication. Cell Res. **22**:1576–1592.
26. **Jäger S, Gulbahce N, Cimermancic P, Kane J, He N, Chou S, D'Orso I, Fernandes J, Jang G, Frankel AD, Alber T, Zhou Q, Krogan NJ.** 2011. Purification and characterization of HIV-human protein complexes. Methods **53**:13–19.
27. **Elias JE, Gygi SP.** 2010. Target-decoy search strategy for mass spectrometry-based proteomics. Methods Mol. Biol. **604**:55–71.
28. **Dunham WH, Larsen B, Tate S, Badillo BG, Goudreault M, Tehami Y, Kislinger T, Gingras AC.** 2011. A cost-benefit analysis of multidimensional fractionation of affinity purification-mass spectrometry samples. Proteomics **11**:2603–2612.